Original article

SARCOIDOSIS VASCULITIS AND DIFFUSE LUNG DISEASES 2025; 42 (4): 17182 DOI: 10.36141/svdld.v42i4.17182

Unveiling CCL2 and CXCL1: Key biomarkers and therapeutic targets in idiopathic pulmonary fibrosis

Jing Pan[1], Guanhua Li[1], Yuanyuan Pu[1], Peilin Li[2], Yan Zhou[3]

[1]Department of Respiratory and Critical Care Medicine, Affiliated Central Hospital of Shandong First Medical University, Jinan, China; [2]Department of Plastic and Cosmetic Surgery, Tsinghua University Yuquan Hospital, Beijing, China; [3]Department of Infectious Diseases, Affiliated Central Hospital of Shandong First Medical University, Jinan, China

Abstract. Idiopathic Pulmonary Fibrosis (IPF) is a chronic, progressive lung disease characterized by fibrosis and impaired lung function. Understanding the molecular mechanisms underlying IPF is crucial for developing effective therapeutic strategies. This study aims to identify differentially expressed genes (DEGs) in alveolar macrophages of IPF patients and validate these findings in an independent cohort. We analyzed gene expression data from the GSE49072 dataset, which includes 23 IPF and 61 normal alveolar macrophage samples. Differential expression analysis was performed using the LIMMA package, and Gene Set Enrichment Analysis (GSEA) identified significant biological pathways. Validation of key DEGs (CCL2, CCL7, and CXCL1) was conducted using ELISA in serum samples from an independent cohort of 50 IPF patients and 50 normal controls. Correlations with clinical parameters such as forced vital capacity (FVC) and diffusing capacity for carbon monoxide (DLCO) were also evaluated. The analysis identified several DEGs, with CCL2 and CXCL1 showing significant upregulation in IPF samples. GSEA highlighted pathways related to inflammatory responses and extracellular matrix remodeling. ELISA validation confirmed elevated serum levels of CCL2 and CXCL1 in IPF patients, correlating with reduced FVC and DLCO. CCL7 did not show significant differences between groups. Targeting these chemokines may offer new therapeutic avenues for IPF treatment. Further research is needed to explore the therapeutic potential and validate findings in larger cohorts. This study enhances our understanding of IPF pathogenesis and identifies promising targets for clinical intervention.

Key words: idiopathic pulmonary fibrosis (IPF), alveolar macrophages, differentially expressed genes (DEGs), biomarkers, inflammatory pathways

Introduction

Idiopathic Pulmonary Fibrosis (IPF) is a chronic, progressive, and ultimately fatal lung disease characterized by the formation of scar tissue within the lungs. This fibrosis leads to a gradual decline in lung function, presenting significant challenges to patients and healthcare providers alike (1). IPF is classified as one of the idiopathic interstitial pneumonias, a group of lung diseases with unknown causes, and it typically affects older adults, with a median survival of 3 to 5 years post-diagnosis (2). The clinical significance of IPF lies in its aggressive nature and the lack of effective treatment options. Patients with IPF experience symptoms such as chronic dry cough, dyspnea (shortness of breath), and fatigue, which severely impact their quality of life (3). The disease's progression is unpredictable; some patients may experience a slow decline, while others face rapid deterioration. Acute exacerbations, periods of sudden worsening of symptoms, are common and often lead to hospitalization and increased

Received: 20 May 2025
Accepted: 25 July 2025
Correspondence:Yan Zhou
Department of Infectious Diseases, Affiliated Central Hospital of Shandong First Medical University, No.105, Jiefang Road, Jinan, Shandong, 250014, China
E-mail: zhouyan5310@163.com
ORCID: 0009-0001-4003-1405

mortality. Current therapeutic strategies for IPF are limited. Antifibrotic agents such as pirfenidone and nintedanib can slow disease progression but do not cure the disease (4). Lung transplantation remains the only definitive treatment, yet it is not suitable for all patients due to age, comorbidities, and the scarcity of donor organs (5). Thus, understanding the pathogenesis of IPF is crucial for developing new, more effective therapies. Alveolar macrophages are specialized immune cells residing in the alveoli, the tiny air sacs in the lungs where gas exchange occurs. These cells play a critical role in maintaining pulmonary homeostasis by clearing inhaled pathogens, particulate matter, and cellular debris. They act as the first line of defense in the respiratory system, orchestrating immune responses and maintaining a balance between pro-inflammatory and anti-inflammatory activities (6). In the context of IPF, alveolar macrophages exhibit altered functionality and phenotypes, contributing to disease pathogenesis. Studies have shown that these macrophages in IPF patients are often polarized towards a profibrotic phenotype (7). This polarization is characterized by the production of fibrogenic cytokines, such as transforming growth factor-beta (TGF-β), and other mediators that promote extracellular matrix (ECM) deposition and fibrosis (8). Furthermore, alveolar macrophages in IPF are involved in aberrant tissue remodeling processes. They interact with epithelial cells, fibroblasts, and other immune cells within the lung microenvironment, exacerbating the fibrotic response. The dysregulated activity of alveolar macrophages not only contributes to the persistence of fibrosis but also hampers effective tissue repair, leading to the progressive nature of IPF. Understanding the specific mechanisms by which alveolar macrophages contribute to IPF is essential for identifying new therapeutic targets. By elucidating the pathways and signals that drive macrophage dysfunction in IPF, researchers can develop strategies to modulate their activity, potentially halting or reversing the fibrotic process. In the current study, we considered differentially expressed genes (DEGs) in a micro-array dataset of patients with IPF compared to normal samples to investigate the involved signaling pathways in this human disease.

Materials and Methods

Data source

The data for this study were retrieved from the Gene Expression Omnibus (GEO) database, specifically the GSE49072 dataset (9). This dataset comprises gene expression profiles of alveolar macrophages from human subjects, including 23 samples from IPF patients and 61 samples from normal controls. The gene expression data were generated using the Affymetrix Human Genome U133A Array platform (GPL96 [HG-U133A]).

Data pre-processing

To ensure the quality and reliability of the microarray data, a series of pre-processing steps was performed. Initially, the raw microarray data underwent background correction to minimize noise and enhance signal quality. Following this, the data were normalized using the normalizeQuantiles method available in the LIMMA (Linear Models for Microarray Data) package within the R/Bioconductor environment (10). This normalization step was crucial to adjust for technical variations and ensure comparability across all samples, converting probe-level data into gene-level expression values.

Differential expression analysis

The identification of differentially expressed genes (DEGs) between IPF patients and normal controls was conducted using the LIMMA package. The analysis process involved several key steps:

- Linear Model Fitting: The lmFit () function was used to fit linear models to the normalized expression data, allowing for the assessment of gene expression differences between the two groups.
- Contrast Definition: The contrastFit () function was employed to define and apply contrasts that specifically test for differences in gene expression between IPF and control samples.
- Statistical Testing: The eBayes () function was applied to compute empirical Bayes statistics, enhancing the reliability and stability of the estimated variances.

DEGs were identified based on an adjusted p-value threshold (<0.01) to account for multiple testing and a minimum |logFC| of 0.5 to ensure biological relevance. This rigorous approach enabled the detection of genes that are significantly upregulated or downregulated in IPF patients compared to normal controls.

Gene Set Enrichment Analysis (GSEA)

To further understand the functional implications of the DEGs, Gene Set Enrichment Analysis (GSEA) was performed using the enrichR package (11). GSEA allows for the identification of significantly enriched biological pathways and processes associated with the DEGs, thereby elucidating the potential mechanisms underlying IPF. The enrichR package was utilized to map the DEGs to predefined gene sets from various databases, including KEGG and Gene Ontology (GO). This mapping provided a comprehensive overview of the biological pathways and processes altered in IPF. The analysis focused on identifying pathways with significant enrichment scores, indicating their relevance to the disease state.

Visualization

The results of the GSEA and the differential expression analysis were visualized using the ggplot2 and pheatmap packages in R. These visualizations facilitated the interpretation of complex data and highlighted key findings. Volcano Plots and Bar Graphs: The ggplot2 package (12) was employed to create volcano plots, which visually represent the significance and magnitude of differential expression for all genes. Additionally, bar graphs were generated to illustrate the top enriched pathways, providing a clear depiction of the most significant biological processes involved in IPF. Heatmaps: The pheatmap package was used to generate heatmaps, displaying the expression patterns of the DEGs across all samples. Heatmaps were particularly useful for visualizing the clustering of gene expression data, highlighting similarities and differences between IPF and normal samples.

Studied population

To validate the identified DEGs from the GSE49072 dataset, we conducted a validation study using an independent cohort. This cohort consisted of 100 subjects, including 50 patients diagnosed with IPF and 50 normal controls. The IPF samples were obtained from the Respiratory Intensive Care Unit (ICU) of Imam Reza Hospital in Tabriz. All participants provided informed consent, and the study was approved by the hospital's ethics committee. The clinical diagnosis of IPF was based on the criteria outlined by the American Thoracic Society/European Respiratory Society (ATS/ERS) guidelines. Control subjects were selected based on the absence of any known pulmonary diseases, ensuring a clear comparison between IPF patients and healthy individuals. Detailed demographic and clinical data were collected for all participants, including age, gender, smoking history, and comorbidities.

ELISA test

To measure the levels of the identified hub genes in the serum of the study population, we employed the Enzyme-Linked Immunosorbent Assay (ELISA) method. Serum samples were collected from all participants and stored at -80°C until analysis. The ELISA kits specific to the identified hub genes were purchased from Thermo Scientific Fisher (USA). The assays were conducted according to the manufacturer's instructions. Briefly, 96-well microplates were coated with capture antibodies specific to the target proteins. Serum samples, standards, and controls were added to the wells and incubated to allow binding of the target proteins. After washing away unbound substances, detection antibodies conjugated with an enzyme were added. Following another incubation and wash cycle, a substrate solution was added to initiate a colorimetric reaction. The intensity of the color, proportional to the concentration of the target protein, was measured using a microplate reader at the 450nm and 570nm.

Statistical analysis

All statistical tests were two-sided, and a p-value of less than 0.05 was considered statistically significant. Analyses were performed using GraphPad Prism v8 (GraphPad Software, Boston, Massachusetts USA, www.graphpad.com) and R v4.2.0. Comparative analysis was performed using the Mann-Whitney U test. Normality was assessed using the Shapiro-Wilk test.

Results

Data pre-processing and quality control

The pre-processing and quality control steps ensured the reliability of the gene expression data from the GSE49072 dataset. This involved background correction, normalization, and summarization of probe-level data into gene-level expressions. Figure 1A shows the normalized expression values for all samples, demonstrating the successful normalization process where expression values are evenly distributed across the samples, indicating effective removal of technical biases. To further assess the quality of the data, Principal Component Analysis (PCA) was performed. PCA helps in visualizing the clustering patterns of samples based on their gene expression profiles. Figure 1B illustrates the PCA plot, where each point represents a sample, and the axes (Dim1 and Dim2) explain the variance in the data. The PCA plot reveals distinct clustering of IPF samples (orange) and normal samples (blue), indicating clear differences in gene expression patterns between the two groups. The percentage of variance explained by each principal component is also indicated on the axes.

Differential expression and pathway enrichment analysis

The differential expression analysis identified a number of genes that were significantly upregulated or downregulated in IPF patients compared to normal controls. Gene Set Enrichment Analysis (GSEA) was subsequently performed to elucidate the biological pathways and processes associated with these DEGs. Figure 2A presents the volcano plot illustrating the differentially expressed genes. Genes with a log2 fold change greater than 0.5 and an adjusted p-value less than 0.01 were considered significantly upregulated (highlighted in red), while genes with a log2 fold change less than -0.5 and an adjusted p-value less than 0.01 were considered significantly downregulated (highlighted in blue). Figure 2B shows the results of the pathway enrichment analysis. The top left panel displays the KEGG pathway analysis, highlighting pathways such as the IL-17 signaling pathway, chemokine signaling pathway, and MAPK signaling pathway, which are significantly enriched in IPF. The other three panels represent the Gene Ontology (GO) enrichment analysis for biological processes, molecular functions, and cellular components. These analyses revealed significant enrichment in processes related to inflammatory response, cytokine activity, and extracellular matrix components, indicating their potential roles in IPF pathogenesis. Figure 2C is a heatmap depicting the expression of genes enriched in the IL-17 signaling pathway across all samples. The heatmap illustrates distinct expression patterns between IPF patients and normal controls, with several genes showing consistent upregulation in IPF samples. Hierarchical clustering of the samples and genes provides further insights into the similarities and differences in gene expression profiles, highlighting potential biomarkers and therapeutic targets.

Demographic and clinical data of validation samples

To validate the results obtained from the *in silico* analysis, we used an independent cohort of 50 IPF patients and 50 normal controls. Of the 50 IPF patients, 25 were receiving antifibrotic therapy (pirfenidone or nintedanib) at the time of sample collection. The remaining patients were either recently diagnosed, unable to tolerate these medications, or awaiting access due to clinical or economic constraints. The demographic and clinical characteristics of the participants are summarized in Table 1. This data provides essential context for understanding the background and health status of the study population, ensuring that the validation results are robust and reliable.

This table highlights the differences and similarities between the IPF and normal control groups in terms of age, gender distribution, smoking status, body mass index (BMI), lung function parameters (FVC and DLCO% predicted), and the prevalence of comorbidities such as hypertension and diabetes. Additionally, the table provides information on the use of medications, specifically corticosteroids and antifibrotic agents, which are commonly prescribed to manage IPF.

Validation of hub gene expression

To validate the *insilico* findings, we measured the serum levels of identified hub genes (CCL2, CCL7, and CXCL1) in the independent cohort consisting of 50 IPF patients and 50 normal controls using the ELISA method. Figure 3 illustrates the

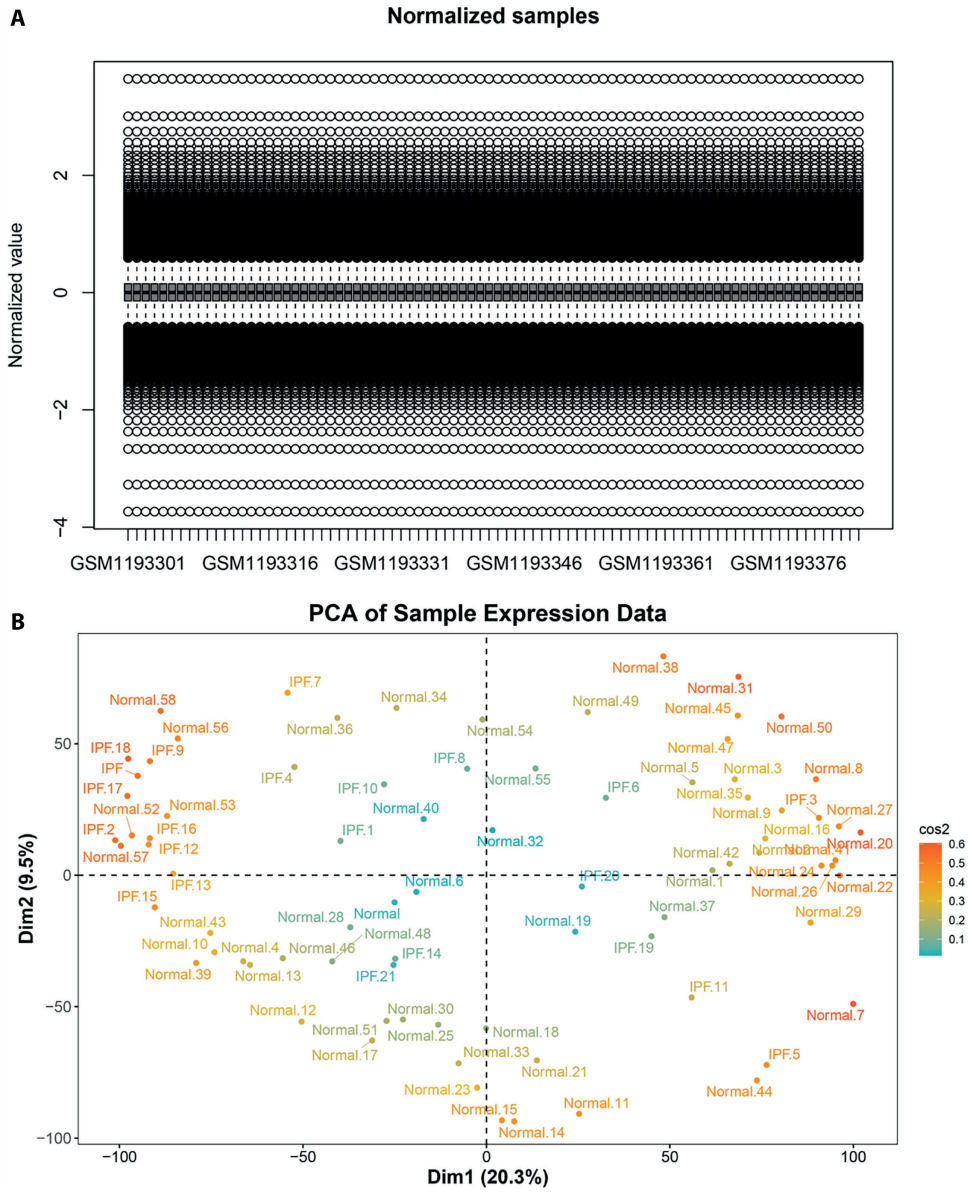

Figure 1. (A) Normalized expression values for all samples from the GSE49072 dataset. The x-axis represents individual samples, and the y-axis shows the normalized expression values. The normalization process ensures that the data is evenly distributed, indicating successful removal of technical biases. (B) Principal Component Analysis (PCA) plot of the sample expression data. Each point represents an individual sample, with IPF samples shown in orange and normal samples in blue. The first principal component (Dim1) accounts for 20.3% of the variance, and the second principal component (Dim2) accounts for 9.5% of the variance. The plot demonstrates clear clustering of IPF and normal samples, reflecting distinct gene expression profiles between the two groups.

comparison of serum levels of these hub genes between the two groups. Subgroup analysis revealed no significant difference in serum levels of CCL2 and CXCL1 between antifibrotic-treated and untreated IPF patients ($p > 0.05$), suggesting that antifibrotic therapy does not confound the observed biomarker expression (Supplementary Figure S1A & S1B). Figure 3A shows the levels of CCL2, which were significantly higher in IPF patients compared to normal controls ($p < 0.0001$). Figure 3B presents the levels of CCL7, which did not show a statistically significant difference between IPF patients and normal controls

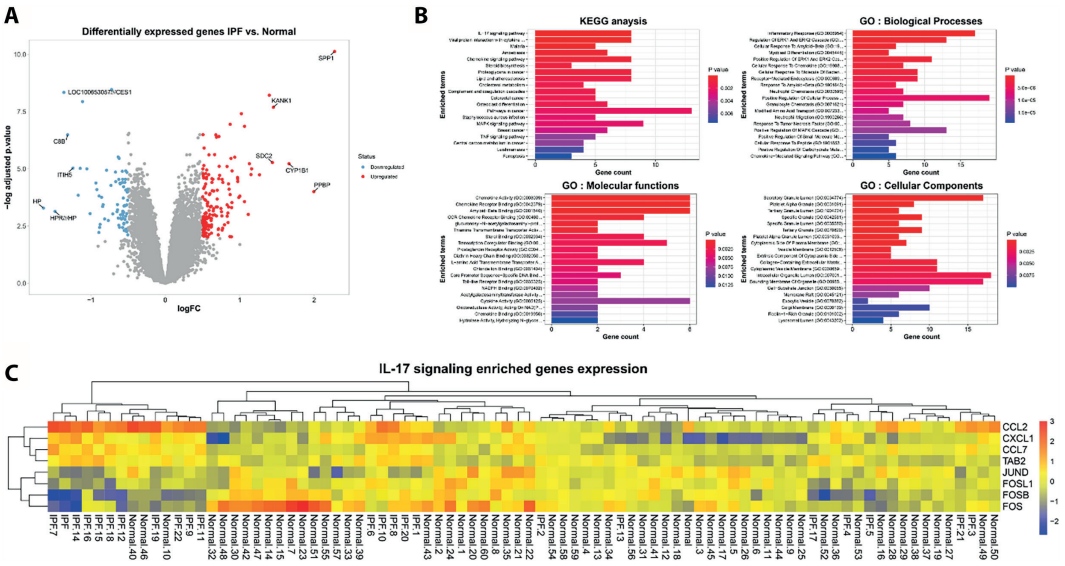

Figure 2. (A) Volcano plot of differentially expressed genes in IPF patients versus normal controls. The x-axis represents the log2 fold change, and the y-axis represents the -log10 adjusted p-value. Genes significantly upregulated in IPF are highlighted in red, and those significantly downregulated are highlighted in blue. Key genes are labeled for reference.(B) Pathway enrichment analysis. The top left panel shows the KEGG pathway analysis, while the other three panels display the GO enrichment analysis for biological processes, molecular functions, and cellular components. The x-axis represents the gene count, and the color gradient indicates the p-value for enrichment.(C) Heatmap of IL-17 signaling pathway enriched genes expression. The heatmap shows the expression levels of key genes across all samples, with hierarchical clustering indicating distinct expression patterns between IPF and normal samples. The color scale represents the normalized expression values, with blue indicating lower expression and red indicating higher expression.

($p > 0.05$). Figure 3C depicts the levels of CXCL1, which were also significantly elevated in IPF patients compared to normal controls ($p < 0.0001$). These results corroborate the in-silico findings and suggest that CCL2 and CXCL1 might serve as potential biomarkers for IPF, while the role of CCL7 needs further investigation. Similarly, serum levels of CCL2 and CXCL1 were not significantly different between corticosteroid-treated and non-treated IPF patients ($p > 0.05$), indicating minimal influence of steroid therapy on these biomarkers (Supplementary Figure-S2).

Correlation of hub gene expression with clinical parameters

To further explore the relationship between the expression levels of the identified hub genes (CCL2, CCL7, and CXCL1) and clinical parameters, we performed a comprehensive analysis involving age, body mass index (BMI), forced vital capacity (FVC), and diffusing capacity of the lungs for carbon monoxide (DLCO). Figure 4 presents a heatmap that integrates the serum levels of the hub genes (in log2 scale) with the clinical data of the patients. The heatmap includes the following variables: Age: Represented in a gradient from yellow (younger) to red (older). BMI: Represented in a gradient from light green (lower BMI) to dark green (higher BMI). FVC (% predicted): Represented in a gradient from light gray (lower FVC) to black (higher FVC). DLCO (% predicted): Represented in a gradient from light pink (lower DLCO) to purple (higher DLCO). The expression levels of CXCL1, CCL2, and CCL7 are shown across samples from both IPF patients and normal controls. The heatmap allows for the visualization of potential correlations between the gene expression levels and clinical parameters. The analysis reveals that elevated levels of CXCL1 and CCL2 are generally associated with IPF patients, who tend to have lower FVC and DLCO percentages. These findings support the notion that CXCL1 and CCL2 may serve as important biomarkers for disease severity and progression in IPF.

Table 1. Demographic and Clinical Data Table for IPF and Normal Samples

Demographic/Clinical Data	**IPF (n=50)**	**Normal (n=50)**
Age (years)	65.4 ± 9.1	64.3 ± 8.5
Gender	25 Male / 25 Female	28 Male / 22 Female
Smoking Status		
Never	12	20
Former	23	15
Current	15	15
BMI (kg/m²)	25.1 ± 4.0	24.8 ± 3.9
FVC % predicted	55.2 ± 12.3	95.6 ± 2.4
DLCO % predicted	45.3 ± 10.8	89.4 ± 5.9
Hypertension	22	15
Diabetes	10	8
Medication Use		
Corticosteroids	18	0
Antifibrotics (e.g., Nintedanib, Pirfenidone)	25	0
Other medications	12	5

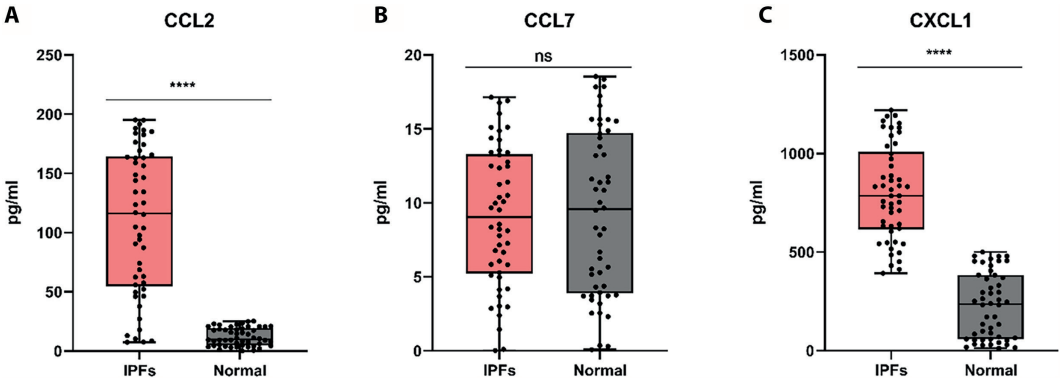

Figure 3. ELISA validation of hub gene expression in serum samples. (A) Serum levels of CCL2 in IPF patients (n=50) and normal controls (n=50). IPF patients show significantly higher levels of CCL2 compared to controls (**** $p < 0.0001$). (B) Serum levels of CCL7 in IPF patients and normal controls. No significant difference was observed (ns: not significant) (C) Serum levels of CXCL1 in IPF patients and normal controls. IPF patients have significantly higher levels of CXCL1 compared to controls (**** $p < 0.0001$). The data are presented as box plots, with each dot representing an individual sample. The horizontal line within each box indicates the median, and the whiskers represent the range of the data.

The relationship between serum chemokine levels and pulmonary function was further explored using correlation analysis. Figure 5 illustrates scatter plots depicting the associations between serum concentrations of CCL2 and CXCL1 and key pulmonary function parameters—forced vital capacity (FVC) and diffusion capacity for carbon monoxide (DLCO). Notably, significant inverse correlations were identified, particularly between CXCL1 and DLCO ($r = -0.52$, $p < 0.001$), suggesting that elevated levels of this chemokine are associated with impaired gas exchange capacity. Similarly, higher CCL2 levels demonstrated negative correlations with both FVC and DLCO, although to a lesser extent. These findings reinforce the potential utility of CCL2 and CXCL1 as surrogate biomarkers

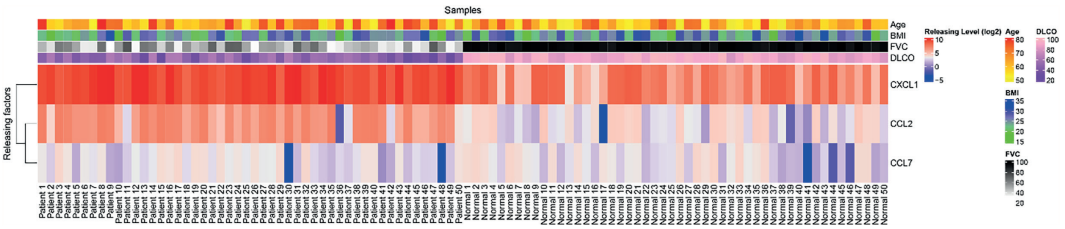

Figure 4. Heatmap illustrating the correlation between the serum levels of hub genes (CCL2, CCL7, and CXCL1) and clinical parameters in IPF patients and normal controls. The heatmap shows: Releasing factors (log2): Expression levels of CXCL1, CCL2, and CCL7. Age: Gradient from yellow (younger) to red (older). BMI: Gradient from light green (lower BMI) to dark green (higher BMI). FVC (% predicted): Gradient from light gray (lower FVC) to black (higher FVC). DLCO (% predicted): Gradient from light pink (lower DLCO) to purple (higher DLCO). Each column represents an individual sample, with the top section showing the clinical parameters and the bottom section displaying the log2 expression levels of the hub genes. The clustering of samples highlights the association of higher gene expression levels with IPF patients, who generally exhibit lower lung function as indicated by FVC and DLCO.

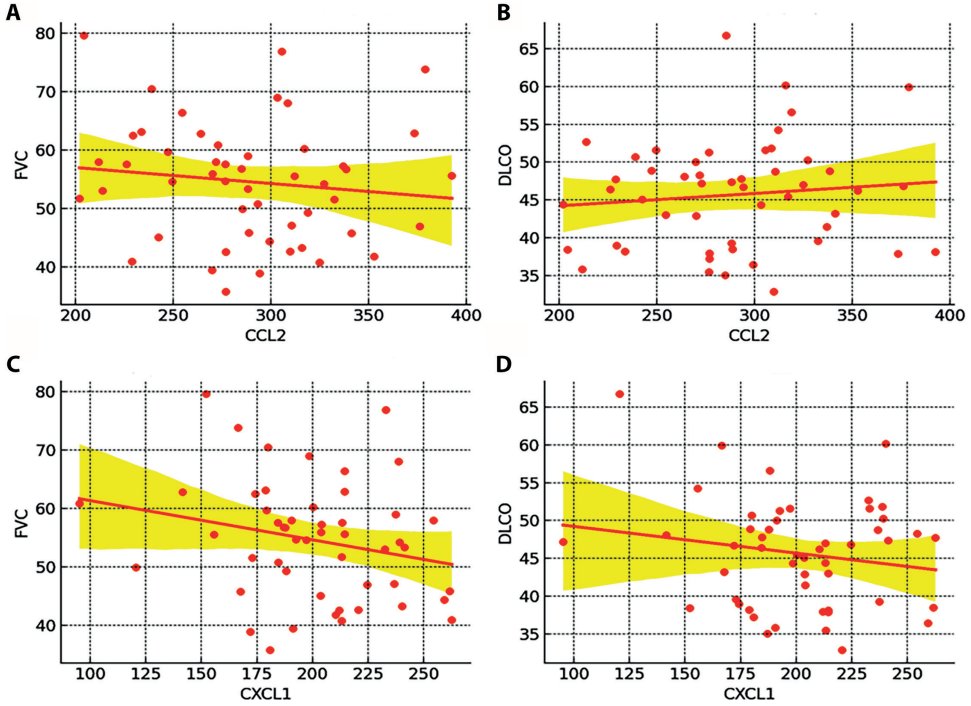

Figure 5. Scatter plots demonstrating correlations between serum biomarker levels and clinical parameters: (A) CCL2 *vs* FVC, (B) CCL2 *vs* DLCO, (C) CXCL1 *vs* FVC, and (D) CXCL1 *vs* DLCO. Significant inverse correlations observed for CXCL1 and clinical metrics ($r \approx -0.52$, $p < 0.001$).

for monitoring disease severity and progression in affected individuals.

Discussion

In this study, we conducted a comprehensive analysis to identify differentially expressed genes (DEGs) in alveolar macrophages of idiopathic pulmonary fibrosis (IPF) patients compared to normal controls using the GSE49072 dataset. Our findings reveal significant alterations in gene expression profiles, providing valuable insights into the molecular mechanisms underlying IPF and potential targets for therapeutic intervention. The differential expression analysis identified several genes that were significantly upregulated or downregulated in IPF patients. Notably, genes such as CCL2, CCL7, and CXCL1 were prominently upregulated, suggesting

their potential role in IPF pathogenesis. The GSEA further highlighted the enrichment of pathways related to inflammatory responses, cytokine activity, and extracellular matrix remodeling, which are known to contribute to the fibrotic process in IPF. To validate these findings, we measured the serum levels of the identified hub genes in an independent cohort of IPF patients and normal controls. The ELISA results confirmed the elevated levels of CCL2 and CXCL1 in IPF patients, while CCL7 did not show a significant difference. These results corroborate our in-silico findings and underscore the potential of CCL2 and CXCL1 as biomarkers for IPF. The elevated levels of CCL2 and CXCL1 in IPF patients highlight their significance in the disease's pathogenesis. CCL2, also known as monocyte chemoattractant protein-1 (MCP-1), is a key mediator in recruiting monocytes and macrophages to sites of inflammation (13). In the context of IPF, increased CCL2 expression can lead to the accumulation of macrophages in the lungs, promoting fibrosis through the secretion of pro-fibrotic cytokines and growth factors (14). CXCL1, a member of the CXC chemokine family, plays a crucial role in neutrophil recruitment and activation (15). Although inflammation is not always considered a prerequisite in IPF pathogenesis, emerging evidence suggests that persistent neutrophilic infiltration, potentially mediated by CXCL1, may exacerbate tissue injury and fibrosis, thereby influencing disease progression (16). Although CCL7 did not show significant differences in our validation cohort, its role in attracting monocytes and eosinophils to sites of inflammation warrants further investigation. The lack of significant differences in CCL7 levels may be due to variability in individual responses or the presence of compensatory mechanisms in IPF patients.

The identification of CCL2 and CXCL1 as potential biomarkers for IPF has significant clinical implications. These biomarkers could be used to develop diagnostic assays for early detection and monitoring of disease progression. Furthermore, targeting these chemokines could offer novel therapeutic strategies for IPF.Several therapeutic approaches could be considered to modulate the activity of CCL2 and CXCL1. Inhibitors of chemokine receptors (e.g., CCR2 for CCL2 and CXCR2 for CXCL1) could potentially reduce the recruitment and activation of inflammatory cells in the lungs, thereby mitigating fibrosis (17). Additionally, neutralizing antibodies or small molecules that specifically block the activity of these chemokines could be explored as therapeutic options. Our study also examined the correlation between the expression levels of hub genes and clinical parameters such as age, BMI, FVC, and DLCO. The heatmap analysis revealed that higher levels of CCL2 and CXCL1 were associated with lower FVC and DLCO percentages in IPF patients. This suggests that elevated expression of these chemokines correlates with impaired lung function and disease severity. These findings emphasize the importance of incorporating molecular biomarkers in the clinical management of IPF. Monitoring the levels of CCL2 and CXCL1 could provide valuable information on disease progression and response to treatment, facilitating personalized therapeutic approaches. Despite the significance of our findings, this study has certain limitations. The validation cohort had a relatively small sample size; however, it is comparable to those used in similar biomarker discovery studies. Importantly, our findings are supported by data from a publicly available dataset, which enhances the reliability and validity of our observations. Nonetheless, larger and more diverse cohorts are needed to further confirm these results. Additionally, the cross-sectional nature of the study precludes the assessment of temporal changes in gene expression and their correlation with disease progression. Future studies should focus on longitudinal analyses to track changes in chemokine levels over time and their association with clinical outcomes. Moreover, exploring the functional roles of CCL2, CXCL1, and other identified DEGs in experimental models of IPF will provide deeper insights into their contributions to the fibrotic process.

Conclusion

Our comprehensive analysis of the GSE49072 dataset has identified significant differentially expressed genes in alveolar macrophages of IPF patients compared to normal controls. Key genes such as CCL2 and CXCL1 were found to be prominently upregulated, highlighting their potential roles in the pathogenesis of IPF. These findings were validated through ELISA measurements in an independent cohort, confirming the elevated serum levels of CCL2 and CXCL1 in IPF patients. The study underscores the importance of CCL2 and CXCL1 as biomarkers for IPF, providing valuable insights into

the molecular mechanisms driving the disease. The correlation of these chemokines with clinical parameters such as FVC and DLCO further emphasizes their potential utility in assessing disease severity and progression. Our results suggest that targeting CCL2 and CXCL1 could offer promising therapeutic strategies for IPF, aiming to mitigate the inflammatory and fibrotic processes that characterize the disease. While further research is needed to explore these therapeutic avenues and validate our findings in larger cohorts, this study lays a solid foundation for future investigations into the molecular underpinnings of IPF and the development of targeted treatments. Overall, our research contributes to a deeper understanding of IPF pathogenesis, offering new perspectives on biomarkers and therapeutic targets that could ultimately improve diagnosis, monitoring, and treatment of this debilitating disease.

Conflict of Interest: Each author declares that he or she has no commercial associations (e.g. consultancies, stock ownership, equity interest, patent/licensing arrangement etc.) that might pose a conflict of interest in connection with the submitted article.

Authors' Contribution: JP, YZ: Conceptualization; JP, GL, YP: Methodology; JP, YP: Validation; JP, GL, PL: Formal analysis; YP, PL: Investigation; JP, GL: Data curation; JP: Writing – original draft; YZ: Writing – review and editing; JP: Visualization; YZ: Supervision; YZ: Project administration. All authors have read and agreed to the published version of the manuscript.

Acknowledgements: The authors declare that no funds, grants, or other support were received during the preparation of this manuscript.

References

1. Sgalla G, Iovene B, Calvello M, Ori M, Varone F, Richeldi L. Idiopathic pulmonary fibrosis: pathogenesis and management. Respir Res. 2018;19(1):32. doi: 10.1186/s12931-018-0730-2.
2. Martinez FJ, Collard HR, Pardo A, et al. Idiopathic pulmonary fibrosis. Nat Rev Dis Primers. 2017;3:17074. doi: 10.1038/nrdp.2017.74.
3. Raghu G. Idiopathic pulmonary fibrosis: lessons from clinical trials over the past 25 years. Eur Respir J. 2017;50(4). doi: 10.1183/13993003.01209-2017.
4. Somogyi V, Chaudhuri N, Torrisi SE, Kahn N, Müller V, Kreuter M. The therapy of idiopathic pulmonary fibrosis: what is next? Eur Respir Rev. 2019;28(153). doi: 10.1183/16000617.0021-2019.
5. George PM, Patterson CM, Reed AK, Thillai M. Lung transplantation for idiopathic pulmonary fibrosis. Lancet Respir Med. 2019;7(3):271-82. doi: 10.1016/s2213-2600(18)30502-2.
6. Joshi N, Walter JM, Misharin AV. Alveolar Macrophages. Cell Immunol. 2018;330:86-90. doi: 10.1016/j.cellimm.2018.01.005.
7. Shi T, Denney L, An H, Ho LP, Zheng Y. Alveolar and lung interstitial macrophages: Definitions, functions, and roles in lung fibrosis. J Leukoc Biol. 2021;110(1):107-14. doi:10.1002/jlb.3ru0720-418r.
8. Krafft E, Lybaert P, Roels E, et al. Transforming growth factor beta 1 activation, storage, and signaling pathways in idiopathic pulmonary fibrosis in dogs. J Vet Intern Med. 2014;28(6):1666-75. doi:10.1111/jvim.12432.
9. Shi Y, Gochuico BR, Yu G, et al. Syndecan-2 exerts antifibrotic effects by promoting caveolin-1-mediated transforming growth factor-β receptor I internalization and inhibiting transforming growth factor-β1 signaling. Am J Respir Crit Care Med. 2013;188(7):831-41. doi:10.1164/rccm.201303-0434OC.
10. Smyth GK. Limma: linear models for microarray data. Bioinformatics and computational biology solutions using R and Bioconductor: Springer; 2005. p. 397-420. doi: 10.1007/0-387-29362-0_23.
11. Kuleshov MV, Jones MR, Rouillard AD, et al. Enrichr: a comprehensive gene set enrichment analysis web server 2016 update. Nucleic Acids Res. 2016;44(W1):W90-7. doi:10.1093/nar/gkw377.
12. Wickham H. ggplot2. Wiley interdisciplinary reviews: computational statistics. 2011;3(2):180-5. doi:10.1002/wics.147.
13. Deshmane SL, Kremlev S, Amini S, Sawaya BE. Monocyte chemoattractant protein-1 (MCP-1): an overview. J Interferon Cytokine Res. 2009;29(6):313-26. doi:10.1089/jir.2008.0027.
14. Gui X, Qiu X, Tian Y, et al. Prognostic value of IFN-γ, sCD163, CCL2 and CXCL10 involved in acute exacerbation of idiopathic pulmonary fibrosis. Int Immunopharmacol. 2019;70:208-15. doi:10.1016/j.intimp.2019.02.039.
15. Korbecki J, Barczak K, Gutowska I, Chlubek D, Baranowska-Bosiacka I. CXCL1: Gene, Promoter, Regulation of Expression, mRNA Stability, Regulation of Activity in the Intercellular Space. Int J Mol Sci. 2022;23(2). doi: 10.3390/ijms23020792.
16. Schupp JC, Binder H, Jäger B, et al. Macrophage activation in acute exacerbation of idiopathic pulmonary fibrosis. PLoS One. 2015;10(1):e0116775. doi: 10.1371/journal.pone.0116775.
17. Horuk R. Chemokine receptor antagonists: overcoming developmental hurdles. Nat Rev Drug Discov. 2009;8(1):23-33. doi:10.1038/nrd2734.

Annex

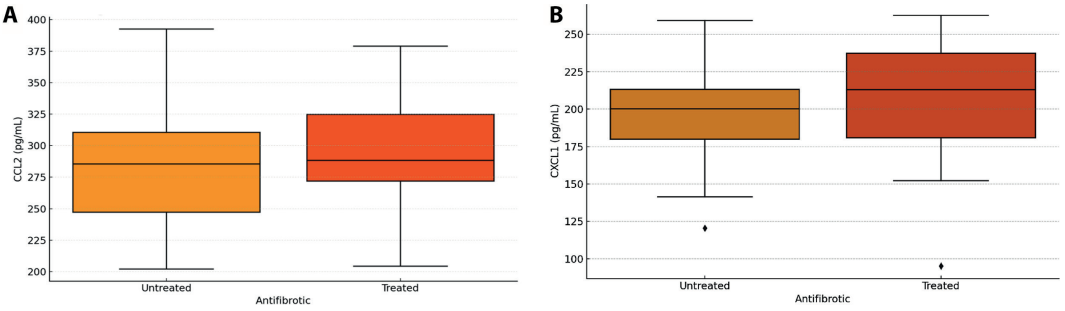

Figure S1. Serum chemokine levels in antifibrotic-treated vs. untreated IPF patients.
(A) Serum levels of CCL2 in antifibrotic-treated vs. untreated IPF patients. No significant difference was observed ($p > 0.05$).
(B) Serum levels of CXCL1 in antifibrotic-treated vs. untreated IPF patients. No significant difference was observed ($p > 0.05$).

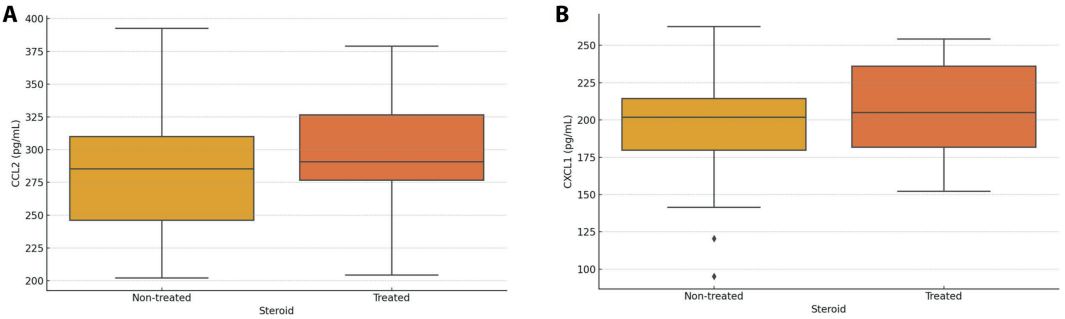

Figure S2. Serum chemokine levels in corticosteroid-treated vs. non-treated IPF patients.
(A) Serum levels of CCL2 in corticosteroid-treated vs. non-treated IPF patients. No significant difference was observed ($p > 0.05$).
(B) Serum levels of CXCL1 in corticosteroid-treated vs. non-treated IPF patients. No significant difference was observed ($p > 0.05$).